

# Three-dimensional tunneling of a diatomic molecule incident upon a potential barrier

Glen L. Goodvin\* and Mark R. A. Shegelski

*Department of Physics, University of Northern British Columbia, Prince George, British Columbia, Canada V2N 4Z9*

(Received 13 July 2005; published 24 October 2005)

We study a diatomic homonuclear molecule incident upon a potential barrier in three dimensions. We study various initial states for the molecule and allow transitions between rotational states of the molecule during the process of tunneling. By applying an elegant method to solve this problem we show that transmission resonances occur in several cases and that adding more binding energy levels for the molecule can tend to decrease the probability of tunneling. We also find that the probability of transmission can be enhanced by the addition of a second potential barrier. These results are in qualitative agreement with those found for the tunneling of a molecule in a one-dimensional model studied previously.

DOI: [10.1103/PhysRevA.72.042713](https://doi.org/10.1103/PhysRevA.72.042713)

PACS number(s): 34.20.Cf, 03.65.Xp, 34.20.Gj, 34.50.Pi

## I. INTRODUCTION

Tunneling in quantum mechanics has been an active area of research for many years. There has been a growing increase in tunneling phenomena due partly to increasing technological advancement. Recently, for example, the tunneling of a single hydrogen atom on a copper surface was observed experimentally [1,2]. The study of the tunneling of a molecule is a fairly new area of research. Resonant tunneling for a pair of bound particles incident upon a single barrier in one dimension has been studied by Saito and Kayanuma [3] and Pen'kov [4,5]. In a recent paper [6] we expanded on their work by including a realistic binding potential that allows transitions between channels (i.e., the energy levels of the binding potential) during the process of tunneling. We applied an elegant approach [7] that accounts for the transitions between channels to solve the problem and considered both a single potential barrier and a pair of potential barriers. In this paper we expand on these works by studying the three-dimensional tunneling of a molecule incident upon a potential barrier. We find that many of the one-dimensional features are reproduced: transmission resonances are obtained, the opening of higher binding energy levels decreases the probability of transmission, and the addition of a second potential barrier can increase the number of transmission resonances. We also find key differences from the one-dimensional tunneling: a molecule incident in its ground state upon a potential barrier in three dimensions demonstrates resonant behavior via a different mechanism than the one-dimensional molecule, the binding energy levels are much more closely spaced due to the inclusion of angular momentum for the molecule, and fewer transmission resonances are found. We also discuss the extension of our work to more realistic experimental settings.

## II. FORMULATION OF THE PROBLEM

We consider a homonuclear molecule of mass  $2m$  incident upon a potential wall  $V(Z)$  in three dimensions as shown in

Fig. 1. By making the potential wall uniform in the plane perpendicular to the direction of the center-of-mass (c.m.) motion we can study three-dimensional tunneling of a molecule in a system where the c.m. motion is one dimensional. This is the simplest choice for a potential barrier in our three-dimensional study. This choice will also allow us to use the elegant method of variable reflection and transmission amplitude discussed later in this section. Using c.m. coordinates the full Hamiltonian for this problem is

$$H = \frac{\mathbf{P}^2}{4m} + \frac{\mathbf{p}^2}{m} + V\left(Z + \frac{1}{2}z\right) + V\left(Z - \frac{1}{2}z\right) + V_0(r) \quad (1)$$

where  $Z$  is the coordinate of the c.m. motion,  $\mathbf{r} = (x, y, z)$  are the coordinates of the relative motion,  $r = \sqrt{x^2 + y^2 + z^2}$  is the magnitude of the separation between the atoms in the molecule,  $V_0(r)$  is the binding potential of the molecule,  $\mathbf{P}$  is the momentum operator for the c.m. motion, and  $\mathbf{p}$  is the momentum operator for the relative motion. We have assumed that the binding potential  $V_0(r)$  depends only on the magnitude of the separation  $r$  between the atoms in the molecule. We will give our choice of  $V_0(r)$  at the beginning of the next section. The relative motion can be broken off from the c.m. motion and solved with

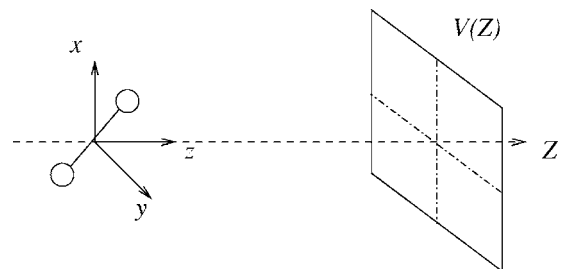


FIG. 1. A homonuclear molecule of mass  $2m$  incident upon a potential wall  $V(Z)$  in three dimensions in the plane perpendicular to the direction of the center-of-mass motion. With this choice of potential the relative motion of the molecule is three dimensional whereas the center-of-mass motion of the molecule is one dimensional.

\*Present address: Department of Physics and Astronomy, University of British Columbia, Vancouver, BC, V6T 1Z1. Electronic Address: [goodving@phas.ubc.ca](mailto:goodving@phas.ubc.ca)

$$\left(\frac{\mathbf{p}^2}{m} + V_0(r)\right)\chi_n(\mathbf{r}) = e_n\chi_n(\mathbf{r}), \quad (2)$$

where  $e_n$  is the binding energy. The relative-motion wave functions  $\chi_n(\mathbf{r})$  can be found with a suitable choice for the binding potential of the molecule. We proceed with a method developed by Razavy [7] by expanding the total wave function  $\Psi(Z, \mathbf{r})$  in terms of the relative-motion wave functions:

$$\Psi(Z, \mathbf{r}) = \sum_{n=0}^{\infty} \psi_n(Z)\chi_n(\mathbf{r}). \quad (3)$$

Substituting this into the full Schrödinger equation  $H\Psi(Z, \mathbf{r}) = E\Psi(Z, \mathbf{r})$  and defining the “effective” potential

$$v_{nm}(Z) = \frac{4m}{\hbar^2} \int_{-\infty}^{\infty} \left[ V\left(Z + \frac{1}{2}z\right) + V\left(Z - \frac{1}{2}z\right) \right] \chi_n^*(\mathbf{r})\chi_m(\mathbf{r})d\mathbf{r} \quad (4)$$

and

$$k_n^2 = \frac{4m}{\hbar^2}(E - e_n), \quad (5)$$

we write the problem as a set of matrix differential equations given by

$$(\nabla^2 + k_n^2)\psi_n(Z) - \sum_m v_{nm}(Z)\psi_m(Z) = 0. \quad (6)$$

We have rewritten the problem in terms of the multichannel Schrödinger equation [7]. This has allowed us to split the two-particle system into two single-particle systems: relative motion and c.m. motion. The effective potential  $v_{nm}$  can be thought of as the potential barrier that the c.m. encounters when incident in channel  $m$  and reflected or transmitted in channel  $n$ , where channel  $i$  denotes the  $i$ th binding energy level of the molecule. The c.m. energy is  $\hbar^2 k_n^2/4m$ .

In order for this paper to be self-contained we will briefly show the steps required to solve for the probabilities of reflection, transmission, and transition between binding energy levels during the process of tunneling. The results are given in Eqs. (15)–(21).

The formal solution of Eq. (6) is

$$\psi_{ni}(Z) = e^{ik_n Z} \delta_{ni} + \frac{1}{2ik_n} \sum_{m=0}^{\infty} \int_{-\infty}^{\infty} e^{ik_n|Z-Z'|} v_{nm}(Z') \psi_{mi}(Z') dZ'. \quad (7)$$

We define

$$R_{ni} = \frac{1}{2ik_n} \sum_{m=0}^{\infty} \int_{-\infty}^{\infty} e^{ik_n Z'} v_{nm}(Z') \psi_{mi}(Z') dZ', \quad (8)$$

$$T_{ni} = \delta_{ni} + \frac{1}{2ik_n} \sum_{m=0}^{\infty} \int_{-\infty}^{\infty} e^{-ik_n Z'} v_{nm}(Z') \psi_{mi}(Z') dZ' \quad (9)$$

as the reflection and transmission coefficients, respectively. Instead of calculating the  $\psi_{ni}$  terms directly and then substituting to find  $R_{ni}$  and  $T_{ni}$ , we follow the method of variable

reflection and transmission amplitude developed by Razavy [7]. To utilize this method we first find the formal solution for the cutoff potential  $v_{nm}(Y, Z)$ ,

$$v_{nm}(Y, Z) = v_{nm}(Z)\theta(Z - Y) \quad (10)$$

where

$$\theta(Z) = \begin{cases} 0, & Z < 0, \\ 1, & Z > 0, \end{cases} \quad (11)$$

and  $Y$  is the cutoff variable for the effective potential (and is not one of the spatial coordinates of the c.m.). The formal solution for this cutoff potential is given by

$$\psi_{ni}(Y, Z) = e^{ik_n Z} \delta_{ni} + \frac{1}{2ik_n} \sum_{m=0}^{\infty} \int_Y^{\infty} e^{ik_n|Z-Z'|} v_{nm}(Z') \psi_{mi}(Y, Z') dZ' \quad (12)$$

for  $Z \geq Y$ ; i.e., just as  $\psi_{ni}(Z)$  is a solution of Eq. (6) with the effective potential  $v_{nm}(Z)$ ,  $\psi_{ni}(Y, Z)$  is a solution of Eq. (6) with  $v_{nm}(Z)$  replaced by the cutoff potential  $v_{nm}(Y, Z)$ . In a similar manner to the definitions (8) and (9) we define

$$R_{ni}(Y) = \frac{1}{2ik_n} \sum_{m=0}^{\infty} \int_Y^{\infty} e^{ik_n Z'} v_{nm}(Z') \psi_{mi}(Y, Z') dZ', \quad (13)$$

$$T_{ni}(Y) = \delta_{ni} + \frac{1}{2ik_n} \sum_{m=0}^{\infty} \int_Y^{\infty} e^{-ik_n Z'} v_{nm}(Z') \psi_{mi}(Y, Z') dZ' \quad (14)$$

as the “variable” reflection and transmission coefficients, respectively [7]. We call these coefficients variable because of their dependence on the variable  $Y$  and they will be used to construct a set of differential equations that can be solved to determine  $R_{ni}$  and  $T_{ni}$ . Note that the subscript  $i$  refers to the incoming channel or binding energy level, whereas the subscript  $n$  refers to the outgoing channel or binding energy level. It is our goal to calculate the reflection and transmission coefficients.

In Ref. [7] it is shown that the problem can be stated as a set of coupled differential equations given by

$$\frac{d}{dY} R_{ni}(Y) = - \sum_{j=0}^{\infty} \frac{1}{2ik_j} [e^{ik_j Y} \delta_{nj} + e^{-ik_j Y} R_{nj}(Y)] \times \sum_{m=0}^{\infty} v_{jm}(Y) [e^{ik_m Y} \delta_{mi} + e^{-ik_m Y} R_{mi}(Y)], \quad (15)$$

$$\frac{d}{dY} T_{ni}(Y) = - \sum_{j=0}^{\infty} \frac{1}{2ik_j} e^{-ik_j Y} T_{nj}(Y) \times \sum_{m=0}^{\infty} v_{jm}(Y) [e^{ik_m Y} \delta_{mi} + R_{mi}(Y) e^{-ik_m Y}] \quad (16)$$

subject to the boundary conditions

$$R_{ni}(Y \rightarrow \infty) = 0, \quad R_{ni}(Y \rightarrow -\infty) = R_{ni}, \quad (17)$$

$$T_{ni}(Y \rightarrow \infty) = \delta_{ni}, \quad T_{ni}(Y \rightarrow -\infty) = T_{ni}. \quad (18)$$

This method will lead to a drastic reduction in the amount of work required in solving for the reflection and transmission coefficients given explicitly in Eqs. (8) and (9). It can be shown that the total probability of reflection for a molecule incident in channel  $i$  is given by

$$p_R^{(i)} = \sum_{n=0}^{\infty} \frac{k_n}{k_i} |R_{ni}|^2 \quad (19)$$

and the total probability of transmission for a molecule incident in channel  $i$  is given by

$$p_T^{(i)} = \sum_{n=0}^{\infty} \frac{k_n}{k_i} |T_{ni}|^2. \quad (20)$$

The probability of transition from one channel to another is found in terms of  $R_{ni}$  and  $T_{ni}$ :

$$P_{i \rightarrow n} = \frac{k_n}{k_i} (|R_{ni}|^2 + |T_{ni}|^2). \quad (21)$$

To test this method we considered a particle incident upon a square barrier in one dimension. This simple problem was solved analytically for  $p_T$  with the usual methods (see, for example, Ref. [8]). We then solved this problem both analytically and numerically using the method of variable reflection and transmission described above. In all three cases the exact same result was obtained for the probability of transmission of the particle. This method was also used in our previous one-dimensional study of the tunneling of a molecule [6].

### III. RESULTS FOR A $\delta$ WALL

We choose the binding potential for the molecule to be an infinite three-dimensional well given by

$$V_0(r) = \begin{cases} \infty, & r < a, \\ 0, & a < r < b, \\ \infty, & r > b, \end{cases} \quad (22)$$

where  $a > 0$ . The radial solutions for this potential are a linear combination of the spherical Bessel functions and Neumann functions and the angular dependence is given by the spherical harmonics [8]

$$\chi_{n\ell m}(\mathbf{r}) = [A j_\ell(q_n r) + B n_\ell(q_n r)] Y_{\ell m}(\theta, \phi) \quad (23)$$

where  $A$  and  $B$  are normalization constants,  $j_\ell(z)$  are the spherical Bessel functions,  $n_\ell(z)$  are the Neumann functions,

$$q_{n\ell}^2 = \frac{m e_{n\ell}}{\hbar^2}, \quad (24)$$

and  $Y_{\ell m}(\theta, \phi)$  are the spherical harmonics. The vanishing of the wave function at  $r=a$  and  $r=b$  and  $\int |\chi_{n\ell m}(\mathbf{r})|^2 d\mathbf{r} = 1$  allows us to determine the eigenvalue conditions and the constants  $A$  and  $B$ . We point out that the energy eigenvalues for the relative motion are closely spaced for increasing angular

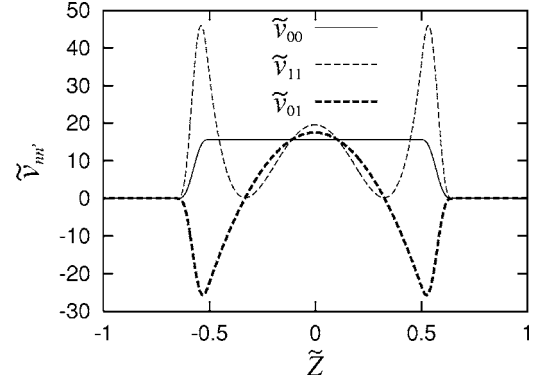


FIG. 2. Effective potentials  $\tilde{v}_{nn'}(\tilde{Z})$  vs  $\tilde{Z}$ . These plots can be thought of as the potential barrier that the c.m. encounters when incident upon the barrier in channel  $n' \equiv n'\ell'm'$  and reflected or transmitted in channel  $n \equiv n\ell m$ . For brevity we have used the index 0 to denote the state 000 and the index 1 to denote the state 020.

momentum and widely spaced for increasing vibrational energy. This is as expected [8].

We choose our external potential to be a  $\delta$  wall of strength  $\lambda$  given by the equation

$$V(Z) = \lambda \delta(Z) \quad (25)$$

and perform the necessary integration to obtain the following expression for the effective potential:

$$v_{nn'}(Z) = \frac{8m\lambda}{\hbar^2} \int \int [\chi_n^*(x, y, 2Z) \chi_{n'}(x, y, 2Z) + \chi_n^*(x, y, -2Z) \chi_{n'}(x, y, -2Z)] dx dy, \quad (26)$$

where we have used  $n\ell m \rightarrow n$  and  $n'\ell'm' \rightarrow n'$  to simplify the notation for the incoming and outgoing channels. To plot the effective potentials we define the following dimensionless parameters:  $\tilde{Z} = Z/a$ ,  $\tilde{k} = ka$ ,  $\tilde{q} = qa$ ,  $\tilde{\chi}_n = a^{3/2} \chi_n$ ,  $\tilde{v}_{nn'} = a^2 v_{nn'}$ ,  $\tilde{\lambda}_n = \lambda_n / (ae_{00})$ , and

$$g = \sqrt{\frac{me_{00}}{\hbar^2}} a. \quad (27)$$

We will use  $q_{00} \approx 10.47$ ,  $q_{02} \approx 10.54$ ,  $g = 15$ ,  $b/a = 1.3$ , and  $\tilde{\lambda} = 0.01$  as the dimensionless parameters throughout the paper (note that these values are not completely arbitrary because of the eigenvalue conditions).

We point out that many of the effective potentials  $v_{nn'}$  are identically zero and therefore the corresponding transition  $n \rightarrow n'$  is forbidden [6]. This occurs due to conservation of parity and conservation of angular momentum in the  $z$  direction. Mathematically, these conservation laws require  $\Delta l = 0, 2, 4, \dots$  and  $\Delta m = 0$  for a transition from channel  $n\ell m \rightarrow n'\ell'm'$ . Therefore, for a molecule incident in its ground state, we must include the states 000, 020, 040, and so on. For brevity we will denote the ground state 000 as 0 and the first excited state 020 as 1.

The integration in Eq. (26) is done numerically and a few of the effective potentials are shown in Fig. 2. The interpretation of these plots is as follows. For the effective potential

$v_{00}$  the molecule is incident and reflected or transmitted in its spherically symmetric ground state  $n\ell m=000$ . In the c.m. frame this amounts to a spherical shell incident upon a  $\delta$  wall, which has the form of a squarelike potential barrier as shown in Fig. 2. The effective potential  $v_{11}$  is similar to the effective potential found in our one-dimensional work. In three dimensions  $v_{11}$  is for incoming and outgoing states both being 020. For the state 020 the molecule is oriented along the  $z$  axis as is expressed by the form of the spherical harmonic  $Y_{20}$  [9]. Here, the  $\delta$  wall has translated into two smooth barriers. The smoothness is a consequence of the integration over the relative motion and the doubling of the barriers occurs because we are looking at the c.m. potential barrier for a quasialigned molecule; the first barrier corresponds to the front particle encountering the  $\delta$  wall and the second barrier corresponds to the back particle encountering the  $\delta$  wall. The three regions from left to right correspond to both particles to the left of the barrier, particles staggering the  $\delta$  wall, and both particles to the right of the barrier, respectively. These features are captured by the well-known lobes of the spherical harmonic  $Y_{20}$  [9]. The effective potential  $v_{01}$  is the potential that the c.m. encounters when it makes a transition from its ground state to its first excited state during the process of tunneling.

With the effective potentials specified we can now calculate the probability that the molecule will tunnel through the  $\delta$  wall. However, because of the nature of the  $v_{nn'}$  terms, we require a numerical method to solve the coupled differential equations given in (13) and (14). We will use a second-order backward Runge-Kutta method.

We first consider a molecule in its ground state  $n\ell m=000$  incident upon the  $\delta$  wall. We include the possibility for a transition to its first excited state  $n\ell m=020$ . For small values of the total energy  $E$  the excited state is unattainable because of energy constraints. It can be shown that the wave number  $k_0$  at which a transition to this state is possible is given by the ‘‘critical’’ wave number

$$k_0^c = \sqrt{\frac{4m}{\hbar^2} \left( \frac{q_{02}}{q_{00}} - 1 \right)} \quad (28)$$

(recall that  $k_0$  is the wave number of a molecule incident in its ground state). When the excited state of the binding potential is unattainable ( $k_0 < k_0^c$ ) both Eqs. (15) and (16) reduce to single differential equations that depend on the ground state of the binding potential only. When the excited state is attainable ( $k_0 \geq k_0^c$ ) both Eqs. (15) and (16) reduce to four coupled differential equations that depend on both the ground state and the first excited state of the binding potential. If we were to include even higher binding potential energies we would need to determine a second critical wave number and solve several more coupled differential equations. For our choice of parameters the critical wave number is  $k_0^c \approx 6.11$ .

We present a plot of the probability of transmission versus incident wave number for a molecule incident in its ground state in Fig. 3. The trend of increasing transmission with higher incident translational energy is clearly seen. Of particular interest is that it is possible to obtain complete trans-

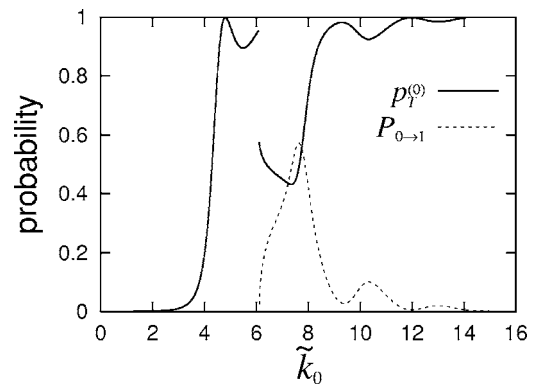


FIG. 3. Probabilities of transmission  $p_T^{(0)}$  and transition  $P_{0 \rightarrow 1}$  versus incident wave number  $\tilde{k}_0$  for a molecule incident upon the  $\delta$  wall in its ground state. Complete transmission is possible even for a small value of  $\tilde{k}_0$ . The molecule incident in its ground state can make a transition to its excited state for values of  $\tilde{k}_0 > \tilde{k}_0^c \approx 6.11$ . The opening of the higher channels *decreases* the probability of transmission as shown by the anticorrelation of the two plots.

mission for a relatively small incident energy. This plot also contains the probability of transition from channel 0 to channel 1 found using Eq. (21). This plot of the probability of transition versus incident wave number shows that the opening of the higher channels *decreases* the probability of transmission. This is because the energy used in exciting the state of the molecule comes at the cost of a decrease in kinetic energy of the molecule, decreasing the chance for transmission. In particular, near the critical wave number a molecule that moves into channel 1 from channel 0 loses almost all of its kinetic energy, leading to an increased probability of reflection for molecules making this transition. Therefore when  $P_{0 \rightarrow 1}$  increases, the probability of transmission decreases in a similar fashion. There is a drop in  $p_T^{(0)}$  at the critical energy due to the opening of the higher channels. Alternatively, a molecule that remains in channel 0 maintains its high kinetic energy and its probability of transmission is very high. We also point out that there are fewer transmission resonances in the three-dimensional result shown in Fig. 3 than in the one-dimensional study [6].

To better understand the plot shown in Fig. 3 we look at the probability of transmission for specific incident states with no transitions. That is, we consider the tunneling of a molecule incident in a state  $n\ell m$  and reflected or transmitted in the same state  $n\ell m$ . Plots of the probability of transmission versus incident wave number for fixed states are given in Fig. 4 for the states  $n\ell m=000$  and  $n\ell m=020$ . By comparing the plots of  $p_T^{(0)}$  in Figs. 3 and 4 it can be seen that the solutions match exactly up until the critical wave number  $\tilde{k}_0^c \approx 6.11$ , as expected since there are no transitions included in the full solution for  $\tilde{k}_0 < \tilde{k}_0^c$ . Beyond the critical wave number the plot of  $p_T^{(0)}$  in Fig. 3 is similar to the plot of  $p_T^{(1)}$  in Fig. 4. This comparison explicitly shows that the resonances beyond the critical wave number in Fig. 3 are primarily due to the nature of the excited state of the molecule; in particular, the quasi-aligned nature of the excited state 020. The curve for the probability of transmission  $p_T^{(1)}$  is very similar

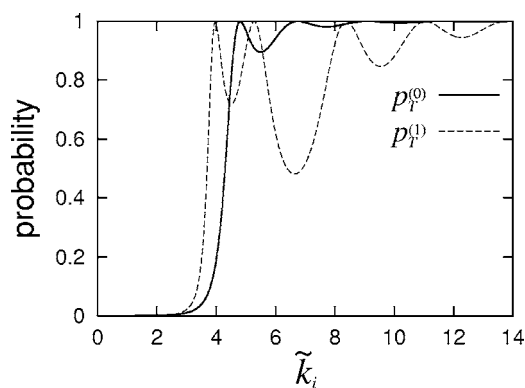


FIG. 4. Probabilities of transmission  $p_T^{(0)}$  and  $p_T^{(1)}$  versus incident wave numbers  $\tilde{k}_0$  and  $\tilde{k}_1$ , respectively, for molecules incident upon the  $\delta$  wall in the fixed states 000 and 020. Comparison of these plots to the full solution shown in Fig. 3 leads to a better understanding of the transmission spectrum. Details are given in the text.

to probability of transmission results reported in the one-dimensional paper [6]. This is again due to the quasialigned nature of the excited state 020.

The physical reason behind the transmission resonances is as follows. In the case of the fixed state result for a molecule incident in its excited state the effective potential consists of a pair of distinct peaks in the c.m. frame as shown in Fig. 2. The resonances are a consequence of destructive interference of the waves reflected at the first peak (i.e., the “front” of the quasialigned molecule) and the waves reflected at the second peak (i.e., the “back” of the quasialigned molecule). For specific incident energies the interference between paths for multiple reflections works constructively and enhances the probability of transmission for the molecule. This phenomenon is similar to what occurs in a Fabry-Pérot interferometer and in antireflection films in optics [10].

The understanding of the resonance for the molecule incident in its ground state is slightly different. The spherically symmetric ground state does not possess the alignment found for the excited state and therefore does not give two distinct peaks for its effective potential. However, due to the square-like nature of the effective potential for this fixed ground state shown in Fig. 2 we can obtain destructive interference between waves reflected from the front of the square barrier and waves reflected from the back of the square barrier. This is analogous to the Ramsauer-Townsend effect [8], which is effectively a resonance condition for a single particle incident upon an attractive square barrier.

We now consider a molecule incident in its excited state. It is necessary to take into account both the ground state and the excited state in this calculation. A plot of  $p_T^{(1)}$  vs  $\tilde{k}_1$  is shown in Fig. 5 (note that  $p_T^{(1)}$  is the total probability of transmission for a molecule incident in its first excited state and  $\tilde{k}_1$  is the wave number for a molecule in its first excited state). We also include  $P_{1\rightarrow 0}$ , the probability of transition from the excited state to the ground state. From this plot we see that the general trend of transmission probability increases to 100% very quickly (i.e., ignoring the resonances) for the excited state because the excited state has the option of moving to the ground state to gain more kinetic energy,

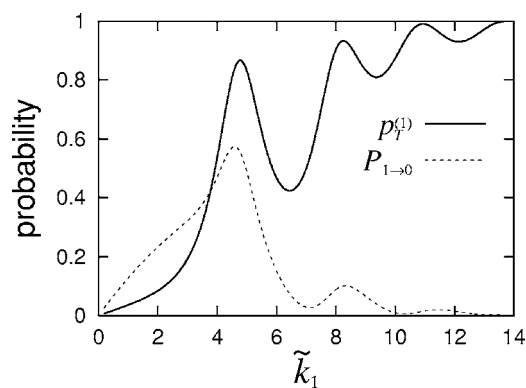


FIG. 5. Probabilities of transmission  $p_T^{(1)}$  and transition  $P_{1\rightarrow 0}$  versus incident wave number  $\tilde{k}_1$  for a molecule incident upon the  $\delta$  wall in its excited state. By moving to its ground state the excited molecule increases its probability of transmission as shown by the correlation between the plots of  $p_T^{(1)}$  and  $P_{1\rightarrow 0}$ .

therefore increasing the probability of tunneling. This statement is further supported by the correlation between the plots of  $p_T^{(1)}$  and  $P_{1\rightarrow 0}$ .

#### IV. RESULTS FOR A PAIR OF $\delta$ WALLS

We next look at the problem of a three-dimensional diatomic molecule incident upon two  $\delta$  walls. The external potential barrier in this case is

$$V(Z) = \lambda_1 \delta(Z) + \lambda_2 \delta(Z - L), \quad (29)$$

where  $\lambda_1$  and  $\lambda_2$  are the strengths of the first and second barriers, respectively, and  $L$  is the separation distance between the  $\delta$  walls. The effective potential for a pair of  $\delta$  walls can be visualized by taking the plot shown in Fig. 2 (which is centered about  $Z=0$  and due to a single  $\delta$  wall) and adding a second single- $\delta$ -wall effective potential centered about  $Z=L$ . The overlap is governed by the separation distance  $L$ . We will look at values of  $L$  large enough such that there is no appreciable overlap between the barrier due to the  $\delta$  wall centered at  $Z=0$  and the  $\delta$  wall centered at  $Z=L$ .

We can apply the same numerical method as in the single- $\delta$ -wall case. We present a plot of probability of transmission versus incident wave number for a molecule in its ground state incident upon a pair of  $\delta$  walls of equal strength  $\tilde{\lambda}_1 = \tilde{\lambda}_2 = 0.005$  separated by a distance  $\tilde{L} = L/a = 2.0$  in Fig. 6. The addition of the second potential barrier gives rise to several more transmission resonances, most notably the strongly peaked resonance at the relatively low wave number  $\tilde{k}_0 \approx 1.92$ . This observation further supports the argument that the resonance behavior found in the study of the tunneling of a molecule is strongly correlated to the existence of multiple peaks in the effective potential.

We are interested in the effects of varying the relative strengths of the two barriers and varying their separation distance. We proceed as before, in the case of a single  $\delta$  wall, to obtain plots of the probability of transmission versus the incident wave number for a molecule in its ground state. We find that identical results are obtained when the strengths of

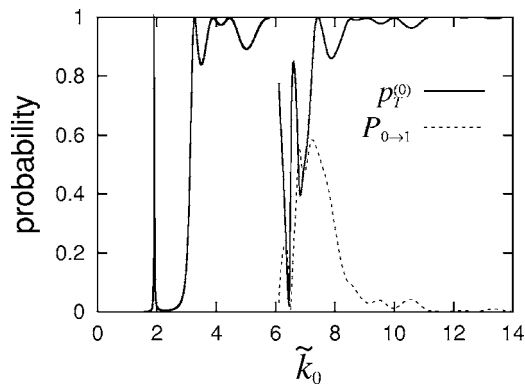


FIG. 6. The probability of transmission  $p_T^{(0)}$  versus wave number  $\tilde{k}_0$  for a molecule in its ground state incident upon a pair of  $\delta$  walls. The strengths of the  $\delta$  walls are  $\tilde{\lambda}_1 = \tilde{\lambda}_2 = 0.005$  and the separation between the barrier is  $\tilde{L} = L/a = 2.0$ .

the barriers are interchanged, as expected. In Fig. 7 we study the effect of varying the relative strengths of the two  $\delta$  walls with  $\tilde{L} \equiv L/a = 2.0$  and maintaining  $\tilde{\lambda}_1 + \tilde{\lambda}_2 = 0.01$ . Note that for  $\tilde{\lambda}_1$  close to 0.01 we are close to reproducing the result from the single- $\delta$ -wall case. We notice that two  $\delta$  walls of equal strength give the highest probability of transmission. This is understood because one expects a molecule to tunnel through two weak barriers with higher probability than tunneling through one strong barrier. The overall structure of the plots in Fig. 7 is very similar to the single  $\delta$  wall case.

We also point out that the value of  $p_T^{(0)}$  has a strong dependence on the separation distance between the barriers due to sensitivity of the results on the length scales involved in this problem.

## V. MORE REALISTIC SYSTEMS

Results for a molecule incident upon a more realistic smooth barrier can also be obtained. In particular, we look at the three-dimensional tunneling of a molecule incident upon a Gaussian barrier given by

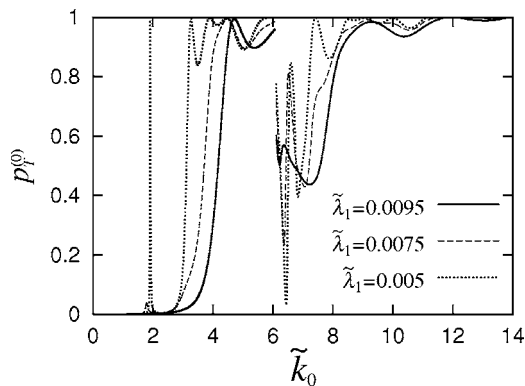


FIG. 7. The probability of transmission  $p_T^{(0)}$  versus wave number  $\tilde{k}_0$  for various relative strengths of the two  $\delta$  walls with  $\tilde{\lambda}_1 + \tilde{\lambda}_2 = 0.01$  and  $\tilde{L} = 2.0$ . The probability of transmission reaches its maximum when the strengths of the two barriers are distributed evenly.

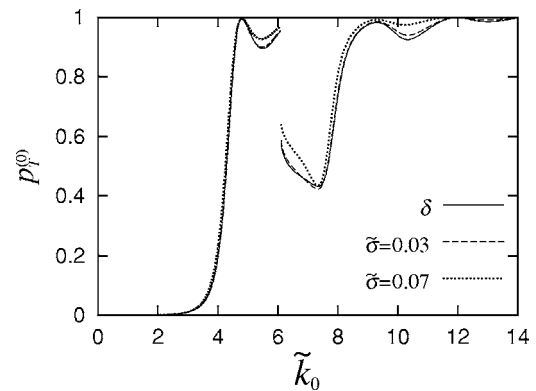


FIG. 8. The probability of transmission  $p_T^{(0)}$  versus wave number  $\tilde{k}_0$  for a molecule incident in its ground state upon Gaussian barriers of varying thicknesses. For values of  $\tilde{\sigma} < 0.03$  the  $\delta$ -wall and Gaussian-barrier results are nearly indistinguishable. For larger Gaussian barrier widths deviation from the  $\delta$ -wall result is found but the important physics is still captured by the  $\delta$ -wall result.

$$V(Z) = \frac{A}{\sigma\sqrt{2\pi}} \exp\left(-\frac{Z^2}{2\sigma^2}\right). \quad (30)$$

We fix the “area” of  $V(Z)$  such that it is equal to the strength  $\lambda$  of the  $\delta$  wall studied previously. This requires that  $A = \lambda$ . The parameter  $\sigma$  (which increases the width of the Gaussian barrier) will be varied to show the deviation between the  $\delta$ -wall result and the Gaussian barrier results.

The effective potential  $v_{nn'}$  is calculated numerically from Eq. (4) and the method of variable reflection or transmission amplitude can be applied to calculate the probability of transmission. We are able to reproduce plots of  $p_T^{(i)}$  vs  $k_i$  almost identical to those shown above in the case of a thin Gaussian barrier that has strength commensurate to the  $\delta$  wall. A plot of the probability of transmission versus incident wave number for a molecule in its ground state incident upon Gaussian barriers of varying thicknesses is given in Fig. 8. These results are plotted together with the  $\delta$ -wall result for comparison.

The results for the probability of transmission are nearly indistinguishable from the  $\delta$ -wall result for  $\tilde{\sigma} = \sigma/a < 0.03$ . For larger Gaussian barrier widths deviation from the  $\delta$ -wall result does occur, as expected. However, we note that even in the case of relatively large Gaussian barrier widths the  $\delta$ -wall result does capture the important physics of this molecular tunneling problem.

Although there are no direct experimental findings on the tunneling of a diatomic molecule through a potential barrier, we point out that there is a strong connection between tunneling problems and scattering problems. Three-dimensional molecular scattering is a current area of experimental research. Examples of recent work in this field include the scattering of  $H_2$  from Cu(001) [11] and NO from diamond(110) [12]. In these studies it is found that some energies are scattered more than others and that the scattering distributions depend on excitations in the rotational and vibrational states of the incident molecule. This is analogous to the transmission resonances presented in both this work and

our previous one-dimensional study [6]. The results presented in both of our three-dimensional and one-dimensional studies could therefore be applied to obtain a qualitative understanding of the physics involved with various molecular scattering experiments.

Recent experimental work has shown that it is possible to align molecules in a molecular beam using laser pulses, optical fields, dc electric fields, and inhomogeneous electric fields [13]. These techniques would permit a step toward a situation where our three-dimensional *and* one-dimensional results could be applied in a realistic experimental setting. The work presented in this paper also has applications in the tunneling of an exciton. For example, in an investigation by Saito and Kayanuma [14], it was shown that a ballistic Wannier exciton exhibits tunneling resonances through a single-barrier heterostructure by the same mechanism as discussed in this paper and our previous one-dimensional study [6]. The methods and results in our investigation could therefore be applied to active areas of experimental and theoretical research involving the tunneling of excitons [15].

## VI. SUMMARY

We have examined the three-dimensional tunneling of a diatomic, homonuclear molecule incident upon a single potential barrier or a pair of potential barriers. We have shown that transmission resonances occur in both cases and that the resonant behavior can be enhanced with the addition of a second potential barrier. The inclusion of higher channels in the binding potential tends to decrease the probability of transmission because the energy used in the excitation results in a decrease in the kinetic energy of the molecule. Alternatively, a molecule incident upon the potential barrier(s) in its

excited state can increase its probability of transmission by moving to its ground state by the same reasoning as above. Plots of the transition probability between the ground state and excited state show this explicitly. In the double- $\delta$ -wall case we found that the interchanging of the barriers yields identical results. We also found that when the sum of the strengths of the two barriers is held constant we obtained the largest probability of transmission for barriers having equal strengths. These features further support the idea that the transmission resonances are a result of destructive interference between the waves reflected from the front barrier and the waves reflected from the back barrier in the c.m. frame. The features discussed above were also found in the case of the one-dimensional tunneling of a molecule studied previously [6]. A key difference between the three-dimensional and one-dimensional tunneling of a molecule is the appearance of an effect analogous to the Ramsauer-Townsend effect for a molecule in its ground state incident upon a potential barrier in three dimensions. We also find fewer transmission resonances in three dimensions than in the one-dimensional case [6]. We have discussed extensions of our results to more realistic systems and the application of our results to the study of tunneling of excitons and molecular scattering. Further studies could include the addition of a more realistic binding potential for the molecule, the inclusion of more bound states for the molecule, or the addition of more external potential barriers.

## ACKNOWLEDGMENTS

This work was supported by the Natural Sciences and Engineering Research Council of Canada (NSERC). One of us (G.L.G.) acknowledges NSERC for partial financial support. We give special thanks to Professor Mohsen Razavy for constructive conversations and helpful suggestions.

- 
- [1] L. J. Lauhon and W. Ho, *Phys. Rev. Lett.* **85**, 4566 (2000).
  - [2] A. Yazdani, *Nature (London)* **409**, 471 (2001).
  - [3] N. Saito and Y. Kayanuma, *J. Phys.: Condens. Matter* **6**, 3759 (1994).
  - [4] F. M. Pen'kov, *J. Exp. Theor. Phys.* **91**, 698 (2000).
  - [5] F. M. Pen'kov, *Phys. Rev. A* **62**, 044701 (2001).
  - [6] G. L. Goodvin and M. R. A. Shegelski, *Phys. Rev. A* **71**, 032719 (2005).
  - [7] M. Razavy, *Quantum Theory of Tunneling* (World Scientific, Singapore, 2003).
  - [8] S. Gasiorowicz, *Quantum Physics*, 2nd ed. (John Wiley & Sons, New York, 1996).
  - [9] *Handbook of Mathematical Functions with Formulas, Graphs, and Mathematical Tables*, edited by M. Abramowitz and I. A. Stegun, 9th ed. (Dover, New York, 1964).
  - [10] F. L. Pedrotti and L. S. Pedrotti, *Introduction to Optics*, 2nd ed. (Prentice Hall, Englewood Cliffs, NJ, 1987).
  - [11] Y. Miura, W. A. Dino, H. Kasai, and A. Okiji, *J. Phys. Soc. Jpn.* **69**, 3878 (2000).
  - [12] C. Roth, J. Hager, and H. Walther, *J. Chem. Phys.* **97**, 6880 (1992).
  - [13] T. P. Rakitzis, A. J. van den Brom, and M. H. M. Janssen, *Science* **303**, 1852 (2004), and references therein.
  - [14] N. Saito and Y. Kayanuma, *Phys. Rev. B* **51**, 5453 (1995).
  - [15] H. Jin H, L. J. Zhang, Z. H. Zheng, X. G. Kong, L. N. An, and D. Z. Shen, *Acta Phys. Sin.* **53**, 3211 (2004), and references therein.